

REPORT DOCUMENTATION PAGE				<i>Form Approved OMB No. 0704-0188</i>	
<small>The public reporting burden for this collection of information is estimated to average 1 hour per response, including the time for reviewing instructions, searching existing data sources, gathering and maintaining the data needed, and completing and reviewing the collection of information. Send comments regarding this burden estimate or any other aspect of this collection of information, including suggestions for reducing the burden, to the Department of Defense, Executive Services and Communications Directorate (0704-0188). Respondents should be aware that notwithstanding any other provision of law, no person shall be subject to any penalty for failing to comply with a collection of information if it does not display a currently valid OMB control number.</small>					
PLEASE DO NOT RETURN YOUR FORM TO THE ABOVE ORGANIZATION.					
1. REPORT DATE (DD-MM-YYYY)		2. REPORT TYPE		3. DATES COVERED (From - To)	
4. TITLE AND SUBTITLE				5a. CONTRACT NUMBER	
				5b. GRANT NUMBER	
				5c. PROGRAM ELEMENT NUMBER	
6. AUTHOR(S)				5d. PROJECT NUMBER	
				5e. TASK NUMBER	
				5f. WORK UNIT NUMBER	
7. PERFORMING ORGANIZATION NAME(S) AND ADDRESS(ES)				8. PERFORMING ORGANIZATION REPORT NUMBER	
9. SPONSORING/MONITORING AGENCY NAME(S) AND ADDRESS(ES)				10. SPONSOR/MONITOR'S ACRONYM(S)	
				11. SPONSOR/MONITOR'S REPORT NUMBER(S)	
12. DISTRIBUTION/AVAILABILITY STATEMENT					
13. SUPPLEMENTARY NOTES					
14. ABSTRACT					
15. SUBJECT TERMS					
16. SECURITY CLASSIFICATION OF:			17. LIMITATION OF ABSTRACT	18. NUMBER OF PAGES	19a. NAME OF RESPONSIBLE PERSON
a. REPORT	b. ABSTRACT	c. THIS PAGE			19b. TELEPHONE NUMBER (Include area code)

PUBLICATION OR PRESENTATION RELEASE REQUEST

Pubkey 962

NRLINST 551 40

15-1231-1228

1. REFERENCES AND ENCLOSURES	2. TYPE OF PUBLICATION OR PRESENTATION	3. ADMINISTRATIVE INFORMATION
Ref: (a) NRL Instruction 5600.2 (b) NRL Instruction 5510.40E Encl: (1) Two copies of subject publication/presentation	<input type="checkbox"/> Abstract only, published <input type="checkbox"/> Book author <input type="checkbox"/> Book editor <input checked="" type="checkbox"/> Conference Proceedings (refereed) <input type="checkbox"/> Journal article (refereed) <input type="checkbox"/> Oral Presentation, published <input type="checkbox"/> Video <input type="checkbox"/> Poster <input type="checkbox"/> Abstract only, not published <input type="checkbox"/> Book chapter <input type="checkbox"/> Multimedia report <input type="checkbox"/> Conference Proceedings (not refereed) <input type="checkbox"/> Journal article (not refereed) <input type="checkbox"/> Oral Presentation, not published <input type="checkbox"/> Other, explain	STRN: NRL/PP/7330-15-2545 Route Sheet No. 7330/ Job Order No. 73-4951-05-5 Classification: U S C FOUO Sponsor: ONR BASE 6.1-Bgr Sponsor's approval: yes* (attached) (*Required if research is other than 6.1/6.2 NRL or ONR unclassified research or if publication/presentation is classified)

URGENT

ALL DOCUMENTS/PRESENTATIONS MUST BE ATTACHED

4. AUTHOR
Title of Paper or Presentation Ocean and Polarization observations from active remote sensing: Atmospheric and Ocean science applications AUTHOR(s) LEGAL NAMES(s) OF RECORD (First, MI, Last), CODE, (Affiliation if not NRL). DAMIEN JOSSET NRC, Weilin Hou 7333, J. Pelon IPSL/LATMOS, Y. Hu NASA/LARC - VA, S. Tanelli Jet Propulsion Laboratory, R. Ferrare NASA Langley Research Center, S. Burton NASA/LARC - VA, Nicolas Pascal ICARE Univ., ICARE team, This paper will be presented at the <u>SPIE DSS</u> (Name of Conference) 20-APR - 24-APR-15, Baltimore, MD, Unclassified (Date, Place and Classification of Conference) and/or for published in <u>SPIE DSS, Unclassified</u> (Name and Classification of Publication)

5. CERTIFICATION OR CLASSIFICATION
It is my opinion that the subject paper (is <u> </u>) (is not <u>x</u>) classified, in accordance with reference (b) and this paper does not violate any disclosure of trade secrets or suggestions of outside individuals or concerns which have been communicated to the NRL in confidence. This subject paper (has <u> </u>) (has never <u>x</u>) been incorporated in an official NRL Report. Weilin Hou, 7333 Name and Code (Principal Author) (Legal Name of Record and Signature Only) (Signature)

6. ROUTING/APPROVAL (NOTE: If name other than your legal name of record is annotated on the publication or presentation itself, add an explanatory note in the "comments" section below next to your signed legal name of record)			
CODE	SIGNATURE	DATE	COMMENTS
Co-Author(s) Weilin Hou, 7333	<i>[Signature]</i>		Need by 20 Apr 2015
Section Head	<i>[Signature]</i>		This is a Final Security Review. Any changes made in the document, after approved by Code 1231, nullify the Security Review.
Branch Head Richard L. Crout, 7330	<i>[Signature]</i>	4-13-2015	
Division Head Ruth H. Preller, 7300	<i>[Signature]</i>	4/13/15	1. To the best knowledge of this Division, the subject matter of this publication (has <u> </u>) (has never <u>x</u>) been classified. 2. This paper (does <u> </u>) (does not <u>x</u>) contain any militarily critical technology.
ADOR/Director NCST E. R. Franchi, 7000			
DOR/CO			
Security, Code 1231	<i>[Signature]</i>	4/17/15	A copy of the paper, abstract or presentation is filed in this office.
Associate Counsel, Code 1008.3	<i>[Signature]</i>	5-8-2015	
Public Affairs (Unclassified/Unlimited Only), Code 7030.4	<i>[Signature]</i>	4-20-15	
Division, Code			
Author, Code			

Ocean and Polarization observations from active remote sensing: Atmospheric and Ocean science applications

Josset¹, W. Hou², J. Pelon³, Y. Hu⁴, S. Tanelli⁵, R. Ferrare⁴, S. Burton⁴, N. Pascal⁶
and the ICARE team⁶

¹ NRC Research Associate at Naval Research Laboratory, Stennis Space Center

² Naval Research Laboratory, Stennis Space Center, MS, USA

³ LATMOS/IPSL, Paris, France

⁴ NASA Langley Research Center, Atmospheric Composition Branch, VA, USA

⁵ Jet Propulsion Laboratory, California Institute of Technology, CA, USA

⁶ ICARE/University Lille 1, Lille, France

ABSTRACT

In the past few years, we have demonstrated how the surface return measured by the active instruments onboard CloudSat and CALIPSO could be used to retrieve the optical depth and backscatter phase function (lidar ratio) of aerosols and ice clouds. This methodology lead to the development of a data fusion product publicly available at the ICARE archive center using the Synergized Optical Depth of Aerosols and Ice Clouds (SODA & ICE) algorithm¹. This algorithm, also allowing to derive ocean surface wind speed, has been extended to include dense cloud surface return to analyze aerosol and cloud properties above such clouds.

This low level data fusion of CALIPSO and CloudSat ocean surface echoes has been used by several researchers to explore different research paths. Among them, we can cite:

- A new characterization of the lidar ratio of cirrus clouds²
- The analysis of the precipitable water and development of a new Millimeter-Wave Propagation Model for the W-Band observations (EMPIRIMA³)
- The analysis of the lidar ratio of sea-spray aerosols⁴, and of Aerosol multilayer lidar ratio and extinction⁵
- A contribution to the retrieval of the subsurface particulate backscatter coefficients of phytoplankton particles⁶

In this paper, we present the main features of SODA & ICE, summarizing some of the results obtained.

Keywords: Lidar, Remote Sensing, Ocean, Aerosols, Clouds

1. INTRODUCTION

Accurate measurements of aerosol and clouds optical properties are required to precisely quantify their radiative effect. Aerosols scatter and absorb solar radiation (direct effect, stronger above highly reflecting surfaces including clouds) and alter the lifetime and development of clouds, which in turn also impact scattering and absorption of radiation (indirect effect).

Among these optical properties, the aerosol optical depth (AOD) is a basic quantity representing the aerosol load in the atmosphere. The main error sources when determining the aerosol optical depth from space are the accuracy of the instrument calibration, the cloud screening algorithm used, the assumption on aerosol microphysical properties

Ocean Sensing and Monitoring VII, edited by Weilin W. Hou, Robert A. Arnone, Proc. of SPIE Vol. 9459
94590N · © 2015 SPIE · CCC code: 0277-786X/15/\$18 · doi: 10.1117/12.2181544

and the different parameterization of the surface⁷. Using the ocean surface echo of CALIPSO and CLOUDSAT altogether, we have developed a new methodology^{8, 9, 10} that allows to overcome the last two issues: CLOUDSAT radar provides a direct measurement of the ocean surface reflectance in the microwave which combined with CALIPSO lidar attenuated surface reflectance in the visible provides a direct retrieval of the total column aerosol attenuation, without any assumption on their type or microphysical properties. It is by definition collocated with CALIPSO/CLOUDSAT vertical information which can be an advantage with respect to passive measurements alone to improve cloud screening. Finally, the measurements are available day and night and above sun glint dominated region. All those characteristics make our methodology an interesting approach to better understand the aerosol radiative effect and its trends. Therefore, aiming at a diffusion to the scientific community, a first version of the product (Synergized Optical Depth of Aerosols and ICE clouds - SODA & ICE) has been created at the French Thematic Center ICARE.

On the basis of recent advancements linked to the use of SODA in ice clouds², W-band radar water vapor absorption³ and feedback from the scientific community, it appears that the first version did not express the whole potential of what could be done with this methodology. This leads to the development of an upgraded version which is now available on the ICARE website. The main objective of this paper is to describe the product and its applications.

2. ALGORITHM DESCRIPTION SODA VERSION 1

GENERAL OVERVIEW

The main goal of the SODA algorithm is to retrieve the optical properties of optically thin atmospheric features over optically dense features. SODA version 1 data product contained the optical depth of semi-transparent aerosols and clouds over the ocean. SODA version 2 now provides the optical depth, the color ratio, and lidar ratio of aerosols and clouds over the ocean and over liquid water clouds.

The concept can be further extended over land¹¹ or to retrieve underwater biological information⁶. These applications are out of the scope of this paper and oceanic applications will only be briefly discussed in the perspectives section of this manuscript.

SODA version 1 is based on a previous publication¹⁰ and the details of the algorithm are presented on the associated website¹. To present the reader with a better understanding of SODA version 2, we will here summarize and illustrate the most relevant elements.

The semi-transparent aerosol and cloud optical depth is retrieved at lidar wavelength through three steps. Only profiles over the ocean are kept in the analysis. In order to emphasize cloud clearing, data profiles are analyzed only if the maximum of the lidar signal is situated at ocean level. This removes profiles with low level dense clouds as well as profiles totally attenuated. As we can see in Fig. 1, most occurrences of the maximum of the surface echo for each orbit are statistically at the ocean surface level. This allows to find the peak of the surface echo.

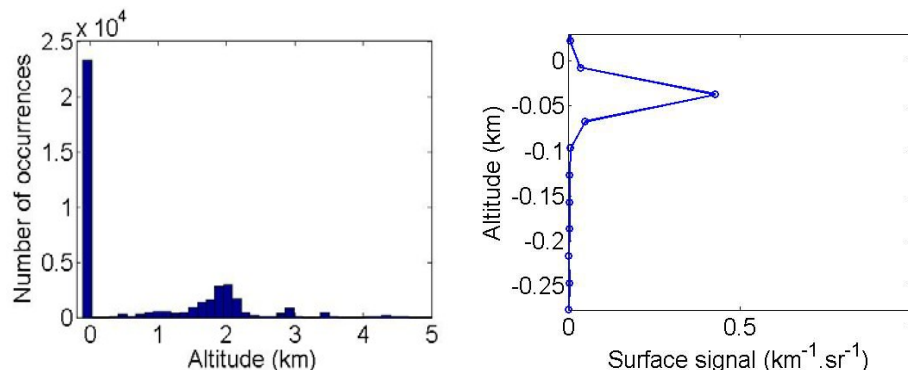


Fig. 1. Left: Distribution of the altitude of the maximum of the surface signal for one orbit of nighttime data (02/09/2009 around 06:53Z). Right: Surface echo used in the integration of the surface signal for one shot around the position 20.22N, -78.30W.

After the position of the maximum has been determined, the integration of the surface signal is performed around this position (Fig. 1). The upper limit includes 2 bins above the peak and the lower limit is determined by the position of the bin number 572 (-0.28 km). This corresponds to the whole energy contained in the surface signal, which is physically consistent with the Bidirectional Reflectance Distribution Function (BRDF)¹².

As we are studying dense surface signal, saturation may happen for the strongest values of the ocean surface signal^{8, 10} and has to be taken into account. The way that has been chosen to filter out saturated signals in SODA V1 is to exclude surface signal which maximum exceeds $2 \text{ km}^{-1} \cdot \text{sr}^{-1}$. The reason behind this choice is the observation of the maximum signal surface distribution (Fig. 2) show a well-defined distribution of values over this threshold. This threshold is higher than the one we discussed in previous studies^{8, 10} and is expected to correspond to the presence of ice (or other solid land surface). When ice is excluded, a partial saturation is still possible and will manifest itself as a loss of linearity of the surface signal at low optical depth. This error source is compensated for in the different processes that we describe below and included in the error budget we previously determined²

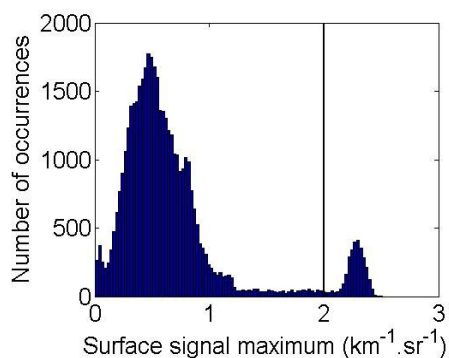


Fig. 2. Distribution of the maximum of the surface signal for one orbit (02/09/2009 around 06:53Z) showing the main surface reflectance distribution over open water and solid surface.

Monthly global calibration (nighttime)

This procedure allows to calibrate the method and through a lidar-radar cross calibration, to correct any monthly calibration bias coming from the lidar or radar. It is based only on the clear-sky observations and does not rely on any underlying assumption of surface roughness behavior.

The first module calculates the 4th order polynomial coefficients linking radar normalized surface scattering cross section σ'_{SR} and the lidar ocean integrated attenuated surface backscatter coefficient $\gamma_{\text{SL,att}}$ (see reference [10], Fig. 1).

This relationship is determined on a monthly basis from collocated nighttime data and only for the clearest lidar profiles (identified as those for which the atmospheric integrated attenuated backscatter coefficient - IAB $< 0.01 \text{ sr}^{-1}$). The radar data are corrected from gaseous water vapor attenuation and from ocean refractive index ρ_{OR} variations with temperature^{13, 10}. Water vapor gaseous attenuation is retrieved from AMSR-E integrated water vapor content using the expression derived by previous research¹⁴. The lidar data are corrected from gaseous attenuation, namely dry air extinction and ozone absorption.

Latitudinal day and night calibration

Potential local calibration biases are then determined by calculating the statistical deviations from the polynomial relationship previously found as a function of latitude. Clear air profiles (IAB $< 0.01 \text{ sr}^{-1}$) are used for both day and night observations (see reference [10], Fig. 4).

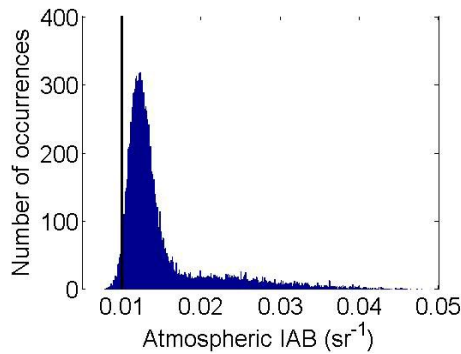


Fig. 3. Atmospheric IAB of all atmospheric features for one nighttime orbit (02/09/2009 around 06:53Z). The black solid line shows the clear air threshold (0.01 sr^{-1}) used in SODA as a limit for clear-air calibration.

Optical Depth retrieval

The remaining deviations from the relationship determined in the previous two steps are then calculated for each shot. The value of the background aerosol optical depth in clearest conditions based on reference [15] gives a baseline value of 0.06 at 532 nm, and 0.04 at 1064 nm to correct the residual AOD. We will discuss this further with the 1064 nm data. The corresponding optical depth of the atmospheric feature is stored into a Hierarchical Data Format (hdf) files along with several control parameters. The same naming conventions than CALIPSO files have been used (an example of file name is SODA_AOD_2010-08-01T01-01-00ZN_V2-02.hdf)

A distinction has to be made at this level between SODA version 1 and SODA version 2. In version 1, only the condition $\text{IAB} < 0.01 \text{ sr}^{-1}$ was removed during the optical depth retrieval process. However, the other filters (saturation and level of the maximum signal) were still active and the corresponding profiles were excluded from the data product. A different approach has been used in SODA version 2, as we will now discuss.

3. FEATURES OF SODA VERSION 2

OVERVIEW

The choice of removing dense features in SODA version 1 was aimed at improving cloud clearing. However, as the underlying principle of the methodology is valid for ice clouds² in SODA version 2, a different approach has been used.

The stages of monthly global calibration and Latitudinal day/night calibration are largely unchanged except for the water vapor correction and for the addition of the calibration of methodology over liquid water clouds (see further). The new water vapor correction has been applied to all steps of the algorithm (see reference [3] for the details of the new parameterization).

For the optical depth retrievals, the filters have been removed and replaced with improved quality flags and scene flags. In version 1, the scene flags were quite basic and allowed some distinction between the aerosols or clouds. In version 2, the scene flag is based on CALIOP vertical feature mask (VFM) and allows the user to select the scene he is interested in (Table 1).

The list of SODA v2 main changes can be summarized as

- New water vapor correction
- more evolved scene flag based on VFM which provides a guidance to discriminate aerosols and their types, ice clouds, water clouds, etc
- More quality flags
- includes dense clouds and aerosols features
- includes lidar ratio retrieval

- Includes optical depth and lidar ratio retrieval over liquid water clouds
- Parameters are determined as in V1 at 532 and 1064 nm, so that color ratios can be further derived.

Table. 1 Scene flag in SODA V2. Bits are numbered from right to left using a little endian coding.

Bit #	6	5	4	3	2	1	0
value	0/1	0/1	0/1	0/1	0/1	0/1	0/1
Criteria	If ice detected in profile						
Signification	type of the highest layer : 0 = Randomly Oriented Ice ; 1 = Horizontally Oriented Ice	Stratospheric feature detected in profile	Liquid water detected in profile	Ice detected in profile	Aerosols detected in profile	Clear profile	Scene Validity

Bit #	14	13	12	9-11	7-8
value	0/1	0/1	0/1	0/7	0/3
Criteria				If aerosol detected	
Signification	AMSR liquid water path > 0 and and <200	Retrievals over liquid cloud available	Retrievals over ocean available	Subtype of the highest layer	Ocean surface type using the Lidar surface depolarization ³¹ : 0=Not determined; 1= liquid water ; 2 = mixed ; 3 = ice

Bit #	19-21	18	17	16	15
value	0/7	0/1	0/1	0/1	0/1
Criteria	If a lower aerosol layer of a different type has been detected	If ice water and aerosol detected in profile	If liquid water detected in profile	If liquid water detected in profile	If liquid water detected in profile
Signification	Subtype of the lower layer	All ice is above the aerosols	Aerosols are present under the lowest liquid bin and no ice clouds found under	All aerosols or cirrus are above the highest liquid bin	All liquid water bins are under the altitude of the 0 Celsius degree isotherm

The approach used in SODA version 2 provides the most flexibility to the user. It is however at the cost of a higher complexity as we can see from the numerous options offered by Table 1. As not all users want to deal with a

complex dataset, a user friendly pre-filtered data product is planned to be made available to the scientific community.

OPTICAL DEPTH RETRIEVAL OVER LIQUID WATER CLOUDS

Over dense liquid water clouds, the cross and co-polarized lidar channels are used as a reference to determine the atmospheric transmission. The algorithm is here also based on the determination of the integrated backscatter but this time dense clouds are used as a target and lidar-only signals are analysed. As we focus on dense clouds as viewed by lidar (typically with $OD > 3$), transmission squared is smaller than 0.005, and the integrated attenuated backscatter coefficient is equal to $\gamma = 1/2S\eta$, where S is the lidar ratio for waterclouds and η the multiple scattering coefficient. This quantity, determined by the size and index of water droplets, has been found to be constant to better than $\pm 5\%$ in most of the clouds.

Depolarization of the lidar signal into liquid water clouds to determine the multiple scattering factor η on which the integrated cloud signal γ depends¹⁶. It had been adapted in SODA algorithm in order to account for the different issues that affect the signal. More specifically, the reason behind this added complexity (described below) is that the data show a deviation from theory (1 to 1 line on Fig. 4 left). Possible reasons are

- Detector transient response¹⁵
- Polarization calibration issues which could come from either the day/night calibration transfer or the low gain/high gain merging process.

The algorithm adjusts the theoretical relationship obtained into liquid water clouds to account for sub-micrometer or non-spherical particles^{16,17,18}, as well as measurement noise, calibration issues and a non-ideal detector transient (Hu et al. cloud phase GRL 2007), using a second order polynomial adjustment as

$$\eta = \eta_{Hu} (\alpha + \beta \eta_{Hu}) \quad (1)$$

Where η_{Hu} is the theoretical relationship^{17,18}. To provide an order of magnitude, in August 2010 the algorithm determined $\alpha = 1.37$ and $\beta = -0.69$ at 532 nm ; $\alpha = 1.22$ and $\beta = -0.61$ at 1064 nm. This modification is further illustrated in Fig. 4 (left figure, curved solid line).

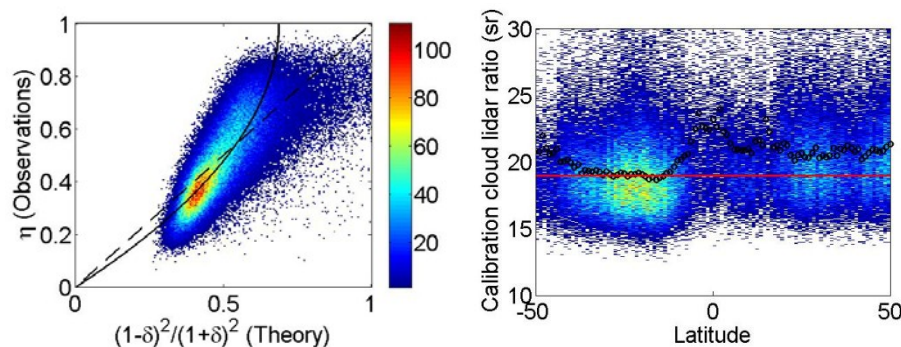


Fig. 4. For August 2010 nighttime data. Left: observed multiple scattering factor for dense liquid water clouds (clear air above) assuming a cloud lidar ratio of 19 sr as a function of the theoretical multiple scattering coefficient (derived from polarized observations). The dotted line is the curve predicted by theory and the solid line is the adjustment performed by the algorithm. Right: derivation of the cloud lidar ratio as a function of latitude, this time using the multiple scattering coefficient from Eq. 1. The black dots show what is used by the algorithm. The red line is at 19 sr.

We determined the depolarization-multiple scattering relationship for all clouds dense enough to be detected on the 333 m cloud level 2 product (which provides top and bottom boundaries). Clouds where the maximum of the

backscatter coefficient in the profile is lower than the cloud base and the cloud liquid water path of AMSR-E is not higher than 0.1 mm were excluded. To remove the uncertainty on the cloud water phase, the cloud top of the cloud layer has to be situated below the isotherm 0°C, as given by the GMAO meteorological data used in the CALIPSO analysis. A lower limit in the integrated backscatter coefficient has been applied so to exclude cloud layers which IAB from cloud top to 20 km was higher than the molecular IAB.

For this case, the average lidar ratio retrieved is 19.4 sr which is very close from the theoretical value (around 19.2 sr over the ocean¹⁷).

Taking into account these constraints in the analysis of the multiple scattering factor and including the modifications with respect of the theoretical relationship for both lidar wavelength, the lidar equation can then be solved unambiguously and optical depth can be retrieved with no assumptions on microphysical properties

LIDAR RATIO ALGORITHM

The lidar ratio used in SODA V2 is the one described previously¹⁹. It has been chosen because of its fast computation speed. Note that there are other ways to solve the Fernald equation^{20, 2, 4}. SODA version 1 opened the door to detailed research on the lidar ratio of specific atmospheric features like cirrus clouds² or marine aerosols⁴ as a function of different geophysical parameters (temperature, wind speed). We hope that the supplemental features of version 2 will allow the scientific community to further explore these topics.

DISCUSSION OF RETRIEVAL UNCERTAINTY

1. The uncertainty of the SODA product over the ocean has been discussed and evaluated in several publications^{8, 10, 2, 3}. The analysis of the CALIPSO/CloudSat ocean surface data points towards an uncertainty in the optical depth that can go as low as $\pm 0.015^3$.

It has to be confirmed observationally that the algorithm retrieval is as accurate as this theoretical limit. The observed dispersion with respect to NASA Langley high spectral resolution lidar (HSRL) flights is equal to around 0.04. This is consistent with our experimental study based on the comparison of SODA with Infrared observations² where we have determined that this error is lower than 0.05.

MODIS is probably the best reference to put these numbers in perspective because of the tremendous amount of work that has been performed for the product validation. For aerosol optical depth τ_{aerL} , MODIS uncertainty over the ocean is $\Delta \tau_{aerL} = \pm 0.03 \pm 0.5 \tau_{aerL}^{21}$.

The uncertainty of the SODA derived cloud or aerosol optical thickness is similar to currently well-established remote sensing products like MODIS and could in theory reach the accuracy of what was aimed by the Glory mission (± 0.02 on optical depth²²). The advantage of SODA is as that the error sources are totally different from passive remote sensing, it can provide interesting complementary information.

2. Still for aerosols, the theoretical error bar of the optical depth over liquid water clouds is around 0.025. This comes from the high theoretical stability of the lidar ratio in liquid water clouds²³. A recent investigation²⁴ proposed that using a constant liquid water clouds lidar ratio in the algorithm could create an error up to 0.1 in the optical depth. The polarization calibration in CALIPSO version 3 seemed to create an artificial day/night polarization bias of around 30%²⁵ which would impact the multiple scattering retrieval. All these effects are taken into account and mitigated by the SODA monthly calibration processes done prior to the optical depth retrieval. Nevertheless, because of the novelty of the method, an exact error budget still has to be derived to evaluate how far is the data product from the theoretical estimate. Comparisons with methodology based on different assumptions^{26, 27} will provide more insight in the matter.
3. For cirrus clouds optical depth τ_{cirL} over the ocean, the lack of well-established reference does not let a lot of choice but to be cautious and provide an error budget that is likely to be overestimated. The total error we have determined for cirrus optical depth based on remote sensing observations is equal to

$\Delta\tau_{cirL} = \sqrt{(0.08)^2 + (0.25\tau_{cirL})^2}$ (see reference [2]). As a reference, optical depth τ_{cloud} of liquid water clouds, which microphysical properties (spherical water droplets) is well understood, MODIS uncertainty is $\Delta\tau_{cloud} = 0.2\tau_{cloud}$. However, a significantly larger, but not clearly quantified, uncertainty exists for COD smaller than 5^{28, 29}. Providing an uncertainty estimate for the optical thickness of cirrus clouds derived from passive sensors is more problematic as the particles forms, shape and roughness vary.

4. Over the ocean, lidar ratios and column AOD derived from CALIPSO lidar data using the SODA technique have been compared with those measured by the NASA Langley Research Center airborne High Spectral Resolution Lidar (HSRL) for several cases of coincident underflights¹⁹. In all the cases studied in reference [19], the average standard deviation between the SODA and HSRL lidar ratios was about 14%. As for liquid water clouds, lidar ratio retrieval from space is a novelty and more work would be useful on the topic. Nevertheless, SODA is as far as we know the only global scale lidar ratio product which is available to the scientific community.

4. PRESENTATION OF THE RESULTS

Contrary to a relatively popular belief, performing a meaningful comparison with AERONET is not straightforward for a track only data product over the ocean. Some insight of the difficulty to compare a track only product with AERONET is provided by a recent study²⁹ (for both land and ocean, issues are magnified over the ocean due to the lower number of data).

We presented in several communications the comparison between SODA, MODIS and POLDER. Overall, the agreement is good. However, the intrinsic differences between MODIS and POLDER make it difficult to reach strong conclusions. In general, SODA version 1 seemed to have a better correlation with POLDER than with MODIS (and more specifically for dust particles) as determined from a few cases but the reverse is found in the data we present here based on SODA version 2 (Fig. 5). Systematic analyses will have to be done to go further. For the month of August 2010 (Fig. 5), SODA optical depth is generally slightly higher than MODIS and lower than POLDER. It may be due to the presence of smoke over the ocean (Fig. 6) which absorption properties are not always easy to retrieve by passive sensors. Several collocated flight with the NASA LaRC HSRL system were performed during this time period and supplemental analysis are underway.

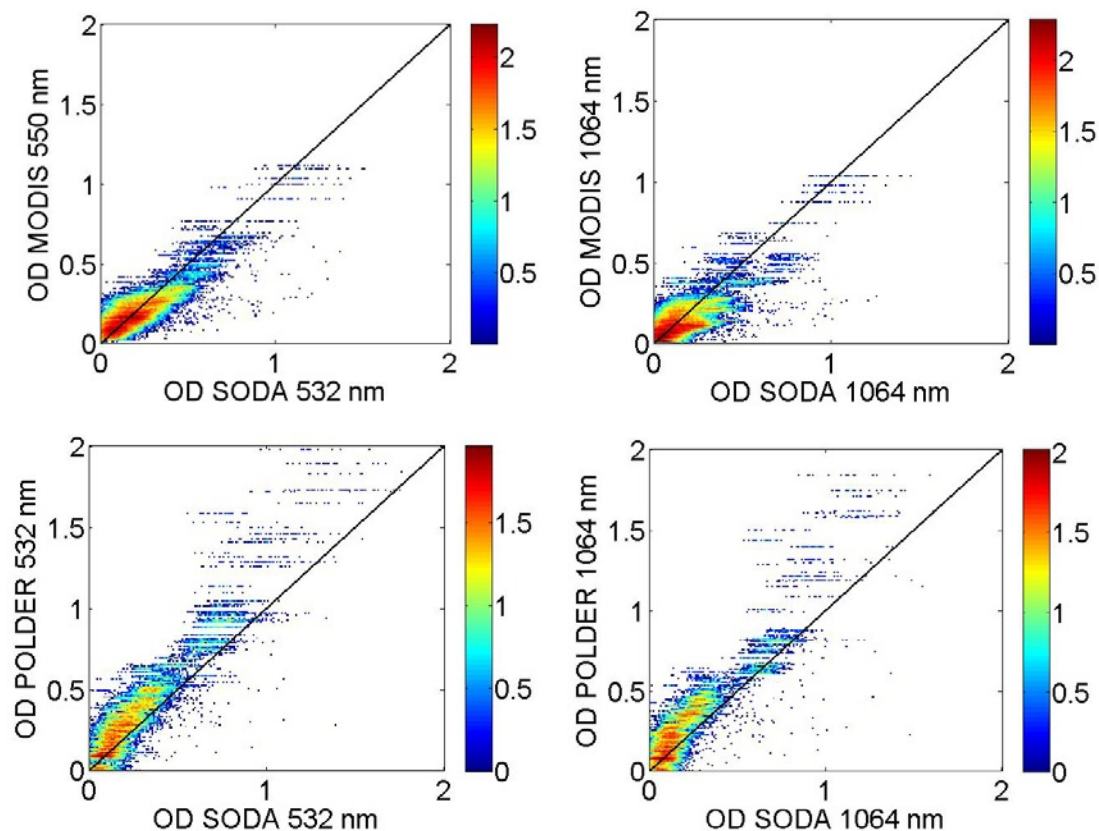


Fig. 5. Upper part: MODIS (collection 5) optical depth as a function of SODA optical depth (532 nm left, 1064 nm right). Bottom part: same figure using the POLDER data. All aerosols (cloud filtered) data over the ocean are used.

Figures 6, 7, 8 and 9 illustrate some results that were obtained from SODA version 2 by filtering the data with the scene flags. The optical depth of dust and smoke (as classified by the VFM) are shown on Fig. 6 over the ocean and on Fig. 7 over liquid water clouds. Fig. 8 and 9 show the same data but for the lidar ratio retrieval. Although maps provide an easy way to illustrate the data, they can sometime provide a false sense of knowledge. For example, the optical depth of dust over the liquid water clouds is very low, and specific attention to details (or alternatively ensure that there is a significant number of data points) would be required before reaching conclusions from the analysis of the optical depth and lidar ratio in that case.

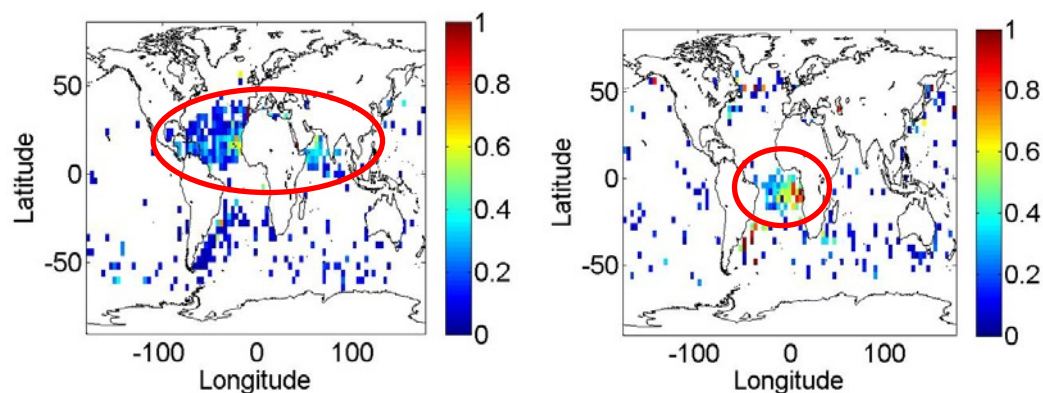


Fig. 6. For August 2010 nighttime data. 532 nm optical depth retrieval for dust (left) and smoke (right). over the ocean. Data have been filtered with the SODA scene flags. The red areas represent where, based on their location, the features appear to be well filtered by the VFM.

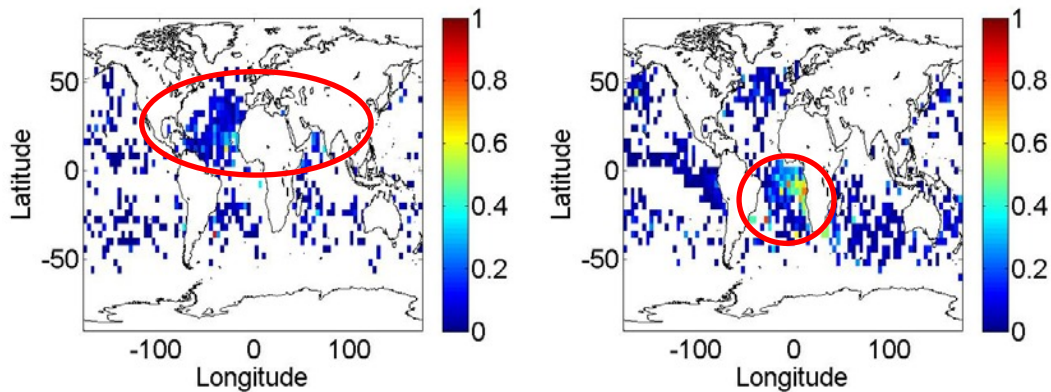


Fig. 7. Same as previous figure but for aerosols above liquid water clouds.

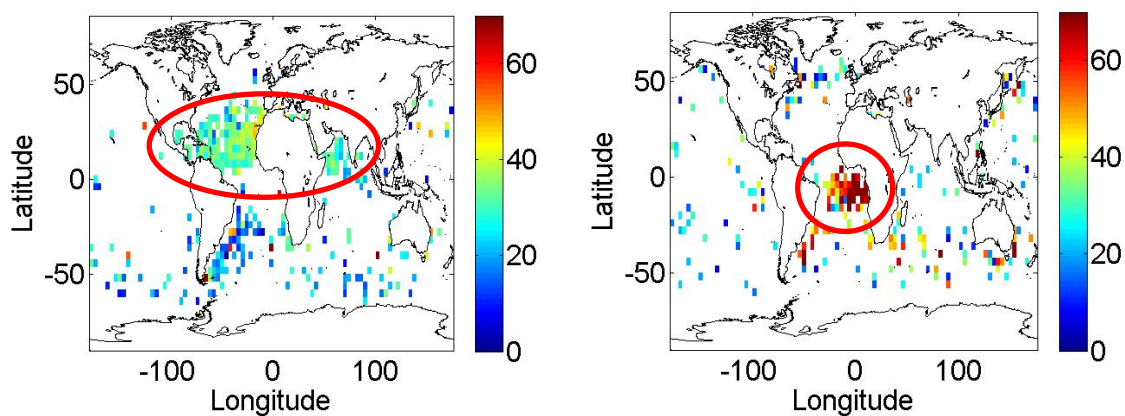


Fig. 8. Same as Fig. 6 but for the 532 nm lidar ratio of dust (left) and smoke (right) over the ocean.

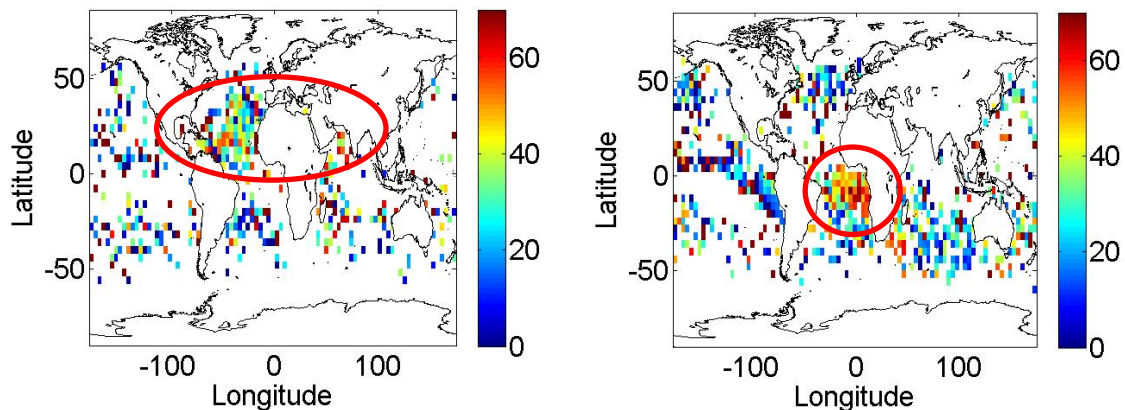


Fig. 9. Same as Fig. 7 but for the 532 nm lidar ratio of dust (left) and smoke (right) above liquid water clouds.

DISCUSSION OF THE 1064 NM LIDAR RATIO

Before concluding this paper, we would like to provide a word of caution about the 1064 nm. The 1064 nm channel calibration uncertainty is higher than the 532 nm. Even if the calibrations processes performed at the different stages of the algorithm mitigate the different error sources, there are less established references at this wavelength (specifically, it is more difficult to validate the 1064 nm data with the HSRL underflights). If the calibration processes work as well at 1064 nm than at 532 nm, the remaining question is to which extent the baseline of optical depth we use¹⁵ is accurate at 1064 nm. An inaccurate baseline will manifest itself as a bias for the lowest 1064 nm

optical depth. If this bias is stable (which has to be for the concept of baseline to be valid), it will be identical for different atmospheric features.

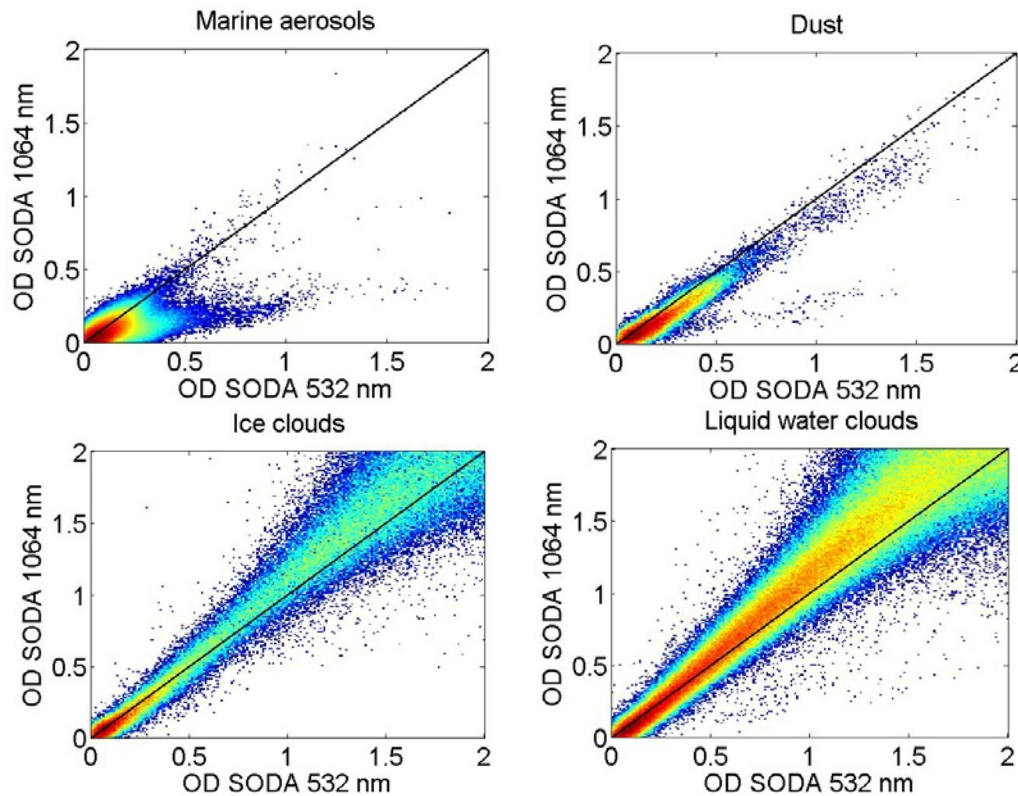


Fig. 10. For August 2010 nighttime. 1064 nm optical depth as a function of the 532 nm optical depth for different kind of atmospheric features. Upper part: marine (left) and dust (right). Bottom: ice (left) and liquid (right) water clouds.

Here we illustrated the concept with coarse mode aerosols and clouds (Fig. 10) as the analysis is more straightforward when we expect some level of wavelength independency. SODA allows to derive the effective OD of semi-transparent layers but the multiple scattering contribution has to be further corrected (note that no multiple scattering corrections are included in SODA). For large particles like liquid water droplets and ice cloud crystals, we can see the effect of the forward peak and of the differential geometry of the lidar emission/reception. The laser light is within the telescope field of view at 532 nm but the laser divergence is larger than the telescope divergence at 1064 nm (see CALIPSO level 1 ATBD table 2.1 note a). When this effect is combined with the larger size of the particle forward peak at 1064 nm, more light escape the telescope at 1064 nm than at 532 nm which creates a slightly larger attenuation (and optical depth). This effect is not noticeable for smaller aerosol particles like dust and marine aerosols. In version 3, smoke aerosols were sometime classified as marine aerosols. It will typically create the “two branches” visible on Fig. 10 for marine aerosols.

Although we do not want to provide a definitive number from this preliminary analysis of one month of data, but it is quite conceivable that the 1064 nm optical depth are slightly underestimated (about 10%) with respect to 532 nm ones. 532 nm seems slightly larger at the lowest optical depth values on Fig. 10. For users interested in the 1064 nm lidar ratio of optically thin features, we suggest a similar analysis to be performed on the optical depth to improve the uncertainty estimate.

CONCLUSION AND PERSPECTIVES

We hope that this short document will help on enlight the reader on the features of the SODA product, its advantages and current limitations.

In term of short term perspectives, further analysis of the atmospheric product (polarization and intensity) will provide insight on atmospheric fine mode fraction and on the use of CloudSat as a reference to correct the underwater lidar polarization observations which has different applications to ocean science⁶.

Long term perspectives are more difficult to foresee. If we look at the past few years, SODA went from what was a concept designed to provide the aerosol optical depth⁸ to applications to aerosols and clouds optical properties (optical depth, color ratio and lidar ratio), water vapor absorption for W-band radar and marine biology.

ACKNOWLEDGEMENTS

This research was performed while the first author held a National Research Council Research Associateship Award at the Naval Research Laboratory, Stennis Space Center. This research was supported by the U.S. Naval Research Laboratory (NRL) and Interagency Agreement IAA (NASA LaRC/NRL) - RPO201513. CNES support and ICARE contribution are acknowledged. NASA, JPL and ICARE provided the data used in this study. ICARE and its support (CNES, CNRS, the Nord-Pas-De-Calais Region and the University of Lille) are greatly acknowledged for performing the operationalization of the SODA product.

REFERENCES

- [1] The SODA project (Synergized Optical Depth of Aerosols) website (<http://www.icare.univ-lille1.fr/projects/soda/>)
- [2] Josset, D., J. Pelon, A. Garnier, Y. Hu, M. A. Vaughan, P. Zhai, R. E. Kuehn, and P. Lucker, Cirrus optical depth and lidar ratio retrieval from combined CALIPSO-CloudSat observations using ocean surface echo. *J. Geophys. Res.*, doi:10.1029/2011JD016959 (2012).
- [3] Josset, D., S. Tanelli, Y. Hu, J. Pelon, P. Zhai, Analysis of water vapor correction for CloudSat W-band radar, *IEEE TGRS*, 51, 7, 3812–3825, doi:10.1109/TGRS.2012.2228659 (2013)
- [4] Dawson, K. W., Meskhidze, N., Josset, D., and Gassó, S.: Spaceborne observations of the lidar ratio of marine aerosols, *Atmos. Chem. Phys.*, 15, 3241–3255, doi:10.5194/acp-15-3241-2015, (2015).
- [5] Ferrare R. and Co-Investigators, NASA ROSES 2012, <https://nspires.nasaprs.com/external/viewrepositorydocument/cmdocumentid=385106/solicitationId=%7B9C00E2B9-561A-63F0-4755-8E5BAC994765%7D/viewSolicitationDocument=1/CCST12%20selections.pdf>
- [6] Behrenfeld, M., Y. Hu, C. Hostetler, G. Dall’Olmo, S. Rodier, J. Hair, and C. Trepte, Space-based lidar measurements of global ocean carbon stocks, *Geophys. Res. Lett.*, 40, 4355–4360, doi:10.1002/grl.50816, (2013).
- [7] Li, Z., Zhao, X., Kahn, R., Mishchenko, M., Remer, L., Lee, K.-H., Wang, M., Laszlo, I., Nakajima, T., and Maring, H.. Uncertainties in satellite remote sensing of aerosols and impact on monitoring its long-term trend: a review and perspective. *Ann. Geophys.*, 27, 2755–2770, doi:10.5194/angeo-27-2755-2009 (2009).
- [8] Josset, D., J. Pelon, A. Protat, and C. Flamant, New approach to determine aerosol optical depth from combined CALIPSO and CloudSat ocean surface echoes, *Geophysical Research Letters*, 35, L10805. doi:10.1029/2008GL033442 (2008)
- [9] Josset, D., J. Pelon, Y. Hu and H. Maring, Determination of aerosol optical properties using ocean reflectance, *SPIE Newsroom*, doi: 10.1117/2.1200903.1574 (2009)
- [10] Josset, D., J. Pelon, and Y. Hu, Multi-instrument calibration method based on a multiwavelength ocean surface model, *IEEE Geoscience and Remote Sensing letter*, 7, 195–199, doi:10.1109/LGRS.2009.2030906 (2010)

- [11] Josset, D., J. Pelon, Y. Hu, P. Zhai, K. Powell, S. Rodier, and C. Trepte, 2010: "CALIPSO Land Surface Mapping Principle and First Results", 25th International Laser Radar Conference (ILRC), St. Petersburg, Russia.
- [12] Josset, D., P. Zhai, Y. Hu, J. Pelon, and P. Lucker, "Lidar equation for ocean surface and subsurface," *Opt. Express* 18, 20862-20875 (2010).
- [13] T. Meissner and F. J. Wentz, "The complex dielectric constant of pure and sea water from microwave satellite observations," *IEEE Trans. Geosci. Remote Sens.*, vol. 42, no. 9, pp. 1836–1849, Sep. 2004.
- [14] S. Tanelli, S. L. Durden, E. Im, K. S. Pak, D. G. Reinke, P. Partain, J. M. Haynes, and R. T. Marchand, "Cloudsat's cloud profiling radar after two years in orbit: Performance, calibration, and processing," *IEEE Trans. Geosci. Remote Sens.*, vol. 46, no. 11, pp. 3560–3573, Nov. 2008.
- [15] Y. J. Kaufman, A. Smirnov, B. N. Holben, and O. Dubovik, "Baseline maritime aerosol: Methodology to derive the optical thickness and scattering properties," *Geophys. Res. Lett.*, vol. 28, no. 17, pp. 3251–3254, Sep. 2001.
- [16] Y. Hu, M. Vaughan, Z. Liu, B. Lin, P. Yang, D. Flittner, B. Hunt, R. Kuehn, J. Huang, D. Wu, S. Rodier, K. Powell, C. Trepte, and D. Winker, "The depolarization - attenuated backscatter relation: CALIPSO lidar measurements vs. theory," *Opt. Express* 15, 5327-5332 (2007).
- [17] Hu, Y., M. Vaughan, D. Winker, Z. Liu, V. Noel, L. Bissonnette, G. Roy, M. McGill, and C. Trepte, 2006: "A Simple Multiple Scattering-Depolarization Relation And Its Potential Application For Space-based Lidar Calibration", 23rd International Laser Radar Conference (ILRC), Nara, Japan.
- [18] X. Cao, G. Roy, N. Roy, and R. Bernier, "Comparison of the relationships between lidar integrated backscattered light and accumulated depolarization ratios for linear and circular polarization for water droplets, fog oil, and dust," *Appl. Opt.* 48, 4130-4141 (2009).
- [19] D. Josset, R. Rogers, J. Pelon, Y. Hu, Z. Liu, A. Omar, and P. Zhai, "CALIPSO lidar ratio retrieval over the ocean," *Opt. Express* 19, 18696-18706 (2011).
- [20] Burton, S. P., et al. (2010), Using airborne high spectral resolution lidar data to evaluate combined active plus passive retrievals of aerosol extinction profiles, *J. Geophys. Res.*, 115, D00H15, doi:10.1029/2009JD012130
- [21] Remer, L. A., Y. J. Kaufman, D. Tanré, S. Mattoo, D. A. Chu, J. V. Martins, R. R. Li, C. Ichoku, R. C. Levy, R. G. Kleidman, T. F. Eck, E. Vermote, and B. N. Holben, 2005, "The MODIS aerosol algorithm, products, and validation," *J. Atmos. Sci.*, vol. 62, no. 4, pp. 947–973.
- [22] Mishchenko, Michael I., and Coauthors, 2007: Accurate Monitoring of Terrestrial Aerosols and Total Solar Irradiance: Introducing the Glory Mission. *Bull. Amer. Meteor. Soc.*, 88, 677–691. doi: <http://dx.doi.org/10.1175/BAMS-88-5-677>.
- [23] R. G. Pinnick, S. G. Jennings, P. Chylek, C. Ham, and W. T. Grandy Jr. Backscatter and extinction in water clouds. *J. Geophys. Res.*, 88 (C11) :6787{6796, 1983.
- [24] Liu, Z., Winker, D., Omar, A., Vaughan, M., Kar, J., Trepte, C., Hu, Y., and Schuster, G.: Evaluation of CALIOP 532 nm aerosol optical depth over opaque water clouds, *Atmos. Chem. Phys.*, 15, 1265-1288, doi:10.5194/acp-15-1265-2015, 2015.
- [25] Sassen, K., and J. Zhu (2009), A global survey of CALIPSO linear depolarization ratios in ice clouds: Initial findings, *J. Geophys. Res.*, 114, D00H07, doi:10.1029/2009JD012279.
- [26] Waquet, F., Riedi, J., Labonnote, L. C., Goloub, P., Cairns, B., Deuzé, J. L., and Tanré, D.: Aerosol remote sensing over clouds using A-train observations, *J. Atmos. Sci.*, 66, 2468–2480, doi:10.1175/2009JAS3026.1, 2009.
- [27] Waquet, F., Cornet, C., Deuzé, J.-L., Dubovik, O., Ducos, F., Goloub, P., Herman, M., Lapyonok, T., Labonnote, L. C., Riedi, J., Tanré, D., Thieuleux, F., and Vanbauce, C.: Retrieval of aerosol microphysical and optical properties above liquid clouds from POLDER/PARASOL polarization measurements, *Atmos. Meas. Tech.*, 6, 991–1016, doi:10.5194/amt-6-991-2013, 2013

- [28] Torres, O., H. Jethva, P. K. Bhartia, 2012: Retrieval of Aerosol Optical Depth above Clouds from OMI Observations: Sensitivity Analysis and Case Studies. *J. Atmos. Sci.*, 69, 1037–1053. doi: <http://dx.doi.org/10.1175/JAS-D-11-0130.1>
- [29] Platnick, S., M. D. King, A. Ackerman, W. P. Menzel, B. A. Baum, J. C. Riedi, and R. A. Frey, 2003: The MODIS cloud products: Algorithms and examples from Terra. *IEEE Trans. Geosci. Remote Sens.*, 41, 459–473.
- [30] Omar, A. H., D. M. Winker, J. L. Tackett, D. M. Giles, J. Kar, Z. Liu, M. A. Vaughan, K. A. Powell, and C. R. Trepte (2013), CALIOP and AERONET aerosol optical depth comparisons: One size fits none, *J. Geophys. Res. Atmos.*, 118, doi:10.1002/jgrd.50330.
- [31] Rodier, S., Y. Hu, and M. Vaughan, 2012: “CALIPSO Surface Return for Ice and Water Detection”, Reviewed & Revised Papers Presented at the 26th International Laser Radar Conference, Papayannis, Balis, and Amiridis, Eds., pp. 801-804